Two-step aminoacylation of tRNA without channeling in Archaea

Hari Bhaskaran[1] and **John J. Perona**[1,2,*]

[1] Department of Chemistry & Biochemistry, University of California, Santa Barbara, CA, USA, 93106-9510

[2] Interdepartmental Program in Biomolecular Science & Engineering, University of California, Santa Barbara, CA, USA, 93106-9510

Abstract

Catalysis of sequential reactions is often envisaged to occur by channeling of substrate between enzyme active sites without release into bulk solvent. However, while there are compelling physiological rationales for direct substrate transfer, proper experimental support for the hypothesis is often lacking, particularly for metabolic pathways involving RNA. Here we apply transient kinetics approaches developed to study channeling in bienzyme complexes, to an archaeal protein synthesis pathway featuring the misaminoacylated tRNA intermediate Glu-tRNA^{Gln}. Experimental and computational elucidation of a kinetic and thermodynamic framework for two-step cognate Gln-tRNA^{Gln} synthesis demonstrates that the misacylating aminoacyl-tRNA synthetase (GluRSND) and tRNA-dependent amidotransferase (GatDE) function sequentially without channeling. Instead, rapid processing of the misacylated tRNA intermediate by GatDE, and preferential elongation factor binding to the cognate Gln-tRNA^{Gln}, together permit accurate protein synthesis without formation of a binary protein-protein complex between GluRSND and GatDE. These findings establish an alternate paradigm for protein quality control via two-step pathways for cognate aminoacyl-tRNA formation.

Keywords

protein synthesis; pre-steady state kinetics; amidotransferase; elongation factor; aminoacyl-tRNA synthetase

Introduction

Channeling of substrates between enzyme active sites provides increased control over metabolic flux, protects labile intermediates from bulk solvent, and allows sequestration of molecular species that may cause toxicity.[1,2] Well-characterized examples of channeling exist in multifunctional enzymes, in which the intermediates pass rapidly through sequestered tunnels prior to reacting in the second active site.[2] Another class of channeling reactions occurs in macromolecular assemblies of two or more components, that are

*To whom correspondence should be addressed. Department of Chemistry & Biochemistry, University of California, Santa Barbara CA 93106-9510. Tel. 805-893-7389; FAX 805-893-4120; perona@chem.ucsb.edu.

Supplementary materials.
Supplementary materials associated with this article can be found online at:

sufficiently stable to permit substrate transfer without dissociation. Purine biosynthesis, the tricarboxylic acid cycle, and mitochondrial respiratory chains are among the diverse pathways for which substrate channeling of this type has been identified.[3–5] Detailed characterization of metabolic channeling is complementary to systems biology efforts to comprehensively describe protein interaction networks *in vivo*,[6,7] since it provides a functional rationale for the formation of binary and higher-order assemblies.

Channeling also occurs in the maintenance and expression of genetic information, where the process involves both protein and nucleic acid components. In particular, channeling of aminoacyl-tRNA for protein synthesis has been demonstrated *in vivo* in transiently permeabilized mammalian cells: exogenously added aminoacyl-tRNAs are unavailable for protein synthesis, while endogenous tRNAs are continuously reutilized.[8,9] This suggests that protein synthesis occurs within a highly organized supramolecular network. Further, in higher eukaryotes nine of the twenty aminoacyl-tRNA synthetases (aaRS) together with three RNA-binding proteins associate in a cytoplasmic multi-tRNA synthetase complex (MSC).[10] Arginyl-tRNA is more efficiently used in protein synthesis when produced by a higher molecular weight form of arginyl-tRNA synthetase (ArgRS) associated with the MSC, as compared with free ArgRS, consistent with a channeling model.[11] Channeling may also occur at other stages of protein synthesis: in the association of aminoacyl-tRNA with elongation factors,[12] in the transport of tRNA out of the nucleus to the ribosome,[13] and in post-translational processes associated with protein folding and translocation.[14, 15]

In lower eukaryotes, bacteria and archaea, associations among aaRS are, so far as is known, limited to smaller assemblies of two to five enzymes.[6,16–18] Further, experiments comparable to those performed on mammalian cells, to examine tRNA channeling *in vivo*, have not been performed. Nonetheless, channeling has been proposed in a variety of contexts, particularly for two-step pathways to cognate aminoacyl-tRNA. In many bacteria, eukaryotic organelles and all archaea, Gln-tRNA^{Gln} and Asn-tRNA^{Asn} synthesis proceeds via formation of a misacylated Glu-tRNA^{Gln} or Asp-tRNA^{Asn} intermediate in a reaction catalyzed by a non-discriminating tRNA synthetase (aaRSND).[19–21] Both GluRSND and AspRSND maintain high selectivity for the cognate amino acid, but each possesses broadened tRNA specificity for two isoacceptor tRNA families (Glu/Gln and Asp/Asn, respectively). Although the structural and mechanistic origins of the broadened tRNA specificity are poorly understood, these enzymes appear very likely to function via a two-step ATP-dependent reaction featuring an activated aminoacyl adenylate intermediate, similar to canonical tRNA synthetases.[22]

The misacylated tRNAs are then converted to Gln-tRNA^{Gln} and Asn-tRNA^{Asn} by tRNA-dependent amidotransferases (AdT).[23,24] Two families of AdT enzymes are known: GatCAB is present in most cells employing the two-step pathway, and can act as both Glu-Adt and Asp-AdT, whereas GatDE is present exclusively in Archaea and functions only with Glu-tRNA^{Gln} as substrate.[23,24] In a three-step reaction, a nitrogen donor (glutamine or asparagine) is first processed by the GatA or GatD subunit to release ammonia, which is then shuttled through an intramolecular tunnel to emerge in the GatB or GatE active site. GatB/GatE binds the misacylated 3′-end of tRNA^{Asn} or tRNA^{Gln}, and phosphorylates the side-chain carboxylate of the esterified amino acid on the tRNA in an ATP-dependent reaction, enabling attack of the translocated ammonia (with release of phosphate) to generate cognate aminoacyl-tRNA.[25–27]

These two-step pathways appear to be prime candidates for channeling, since sequestration of misacylated tRNA could alleviate possible toxicity associated with misincorporation into protein. Indeed, recent crystal structures of ternary GatCAB:AspRSND-tRNA^{Asn} and GatCAB:GluRSND-tRNA^{Gln} complexes have directly demonstrated formation of a

macromolecular assembly between the tRNA substrate and the two enzymes, corroborating prior observation of ternary protein-tRNA complexes in solution.[28–30] These data provided the basis for postulating the existence of a "transamidosome", which is proposed to directly channel misacylated tRNAs from the aaRS[ND] to GatCAB. The model for function includes unimolecular conformational rearrangements in this ternary complex, by which the tRNA 3′-end is redirected from the GluRS[ND] active site to that of GatCAB while maintaining binding.[30] Although crystal structures of ternary complexes have not been determined in the GatDE system, biochemical evidence for GluRS[ND]-GatDE and GluRS[ND]-GatDE-tRNA[Gln] binary and ternary complex formation has been reported.[31] Molecular modeling based on the GatCAB ternary complexes was also used to infer that ternary complex formation by GatDE is plausible.[30]

Although formation of complexes is consistent with the notion of substrate channeling, explicit transfer of misacylated tRNA from aaRS[ND] to the amidotransferase has not been demonstrated for any two-step aminoacylation pathway. Thus, the possibility remains that misacylated tRNA dissociates into solution prior to rebinding the amidotransferase. In the GatDE experiments, the proposed GatDE-GluRS[ND] binary complex is apparently unstable during the course of the reaction, and neither GluRS[ND] nor GatDE is reported to affect the activity of its partner enzyme.[31] Hence, alternative mechanisms to maintain protein quality control and to avoid potential toxicity of misacylated tRNA, in the absence of channeling, must be considered.

To provide a more definitive interrogation of channeling in two-step aminoacyl-tRNA synthesis, we have applied pre-steady state kinetic approaches developed in our laboratory for the study of discriminating aaRS,[32] to the two-step GluRS[ND]-GatDE pathway from *Methanothermobacter thermautotrophicus* – which was also the subject of the prior analyses.[27,31] Our experimental approach relies on applying the strategy developed for study of bifunctional enzymes such as thymidylate synthase – dihydrofolate reductase,[33] where channeling was demonstrated by comparing and analyzing separate rapid kinetics measurements for each independent enzyme and for the full two-step reaction. Other studies taking this approach have demonstrated the absence of channeling in systems where its existence had been presumed.[34] By combining these measurements with kinetic simulations, we have generated a comprehensive thermodynamic and kinetic scheme for the two-step pathway, which demonstrates to a high degree of confidence that the GluRS[ND] and GatDE function independently and that the misacylated tRNA is not sequestered. Thus, in contrast to the earlier findings,[31] our data do not support the existence of a GatDE transamidosome in Archaea. Instead, we suggest that specific and rapid ATP-dependent conversion of Glu-tRNA[Gln] to Gln-tRNA[Gln] by GatDE, and binding of translation elongation factor 1α (EF-1α) to Gln-tRNA[Gln] and not to Glu-tRNA[Gln], together provide sufficient discrimination against delivery of Glu-tRNA[Gln] to the ribosome. These experiments offer the first definitive evaluation of channeling for any RNA-based metabolic pathway.

Results

Kinetic dissection of Gln-tRNA[Gln] formation

Our strategy for detailed study of the GluRS[ND]-GatDE pathway consists of performing three sets of pre-steady state kinetics experiments. First, we measure the maximum rate constant (k_{max-1}) for GluRS[ND]-mediated Glu-tRNA[Gln] formation from tRNA[Gln] in single turnover reactions (Fig. 1). Next, we perform analogous experiments to measure k_{max-2} for GatDE-mediated Gln-tRNA[Gln] formation from Glu-tRNA[Gln]. Finally, we monitor formation of Glu-tRNA[Gln] and Gln-tRNA[Gln] in the presence of both GluRS[ND] and GatDE, on timescales permitting observation of a Glu-tRNA[Gln] intermediate if it indeed accumulates. Further measurements of second-order association steps and first-order dissociation steps are also

made. We employ a reaction scheme incorporating these rate constants and build models for both channeled and dissociative pathways using kinetic simulations. Comparison of simulated plots and observed data then allows distinguishing a two-step dissociative mechanism from channeling mechanisms, as demonstrated previously for small-molecule metabolites in bifunctional enzymes.[33,34] If direct channeling obtains, the simplest expectations are that the formation of Gln-tRNA^{Gln} is limited only by the formation of Glu-tRNA^{Gln} (k_{max-1}), and that no accumulation of the Glu-tRNA^{Gln} intermediate in the presence of both enzymes will be observed (Fig. 1a). In contrast, accumulation of Glu-tRNA^{Gln} would suggest lack of channeling.

Rapid release of Glu-tRNA^{Gln} product from GluRSND

We began by dissecting the steps of Glu-tRNA^{Gln} formation by GluRSND, employing kinetic approaches similar to those developed for quantitative characterization of *E. coli* GlnRS in our laboratory (Fig. 2).[32] Product formation with time was monitored in single turnover reactions with molar excess of GluRSND over tRNA^{Gln}, at varying concentrations of enzyme, and at saturating ATP and glutamate concentrations (10 mM and 50 mM, respectively) (Fig. 2b). Replots of this data revealed a linear dependence of k_{obs} with GluRSND concentration under subsaturating conditions, allowing extraction of a second-order rate constant. The numerical value of this constant, 2.6×10^6 M^{-1}sec^{-1}, is equivalent to the k_{cat}/K_m that we previously reported by monitoring steady-state reactions (Fig. 2c – shaded portion).[35] This value places a lower limit on the second-order rate constant for binding (k_{on}) of GluRSND to tRNA^{Gln} in the forward reaction pathway. At higher concentrations of GluRSND, saturation is observed (Fig. 2c). The k_{max} of 0.12 sec^{-1} is identical within error to the previously determined k_{cat},[35] suggesting that either the rate of the chemical steps on the enzyme, or a first-order conformational rearrangement prior to catalysis, is rate-limiting for the reaction. These data also allow determination of the equilibrium dissociation constant for tRNA at 40 nM, identical to the value previously reported based on fluorescence anisotropy measurements of the binary complex.[31] We also find that inclusion of GatDE in GluRSND single-turnover reactions, at equimolar concentration, does not influence the rate of product formation (data not shown).[31]

To further evaluate the hypothesis that an early step is rate-limiting, we monitored product formation under conditions that would allow observation of a pre-steady state burst followed by multiple turnovers. No burst was observed at 500 nM enzyme and 5–10 μM tRNA^{Gln}, and linear fits to the data allowed derivation of k_{cat} identical to that obtained in steady-state kinetics (Fig. 2d).[35] The absence of a characteristic burst at either tRNA^{Gln} concentration confirms that Glu-tRNA^{Gln} dissociation from GluRSND occurs rapidly and is not rate-limiting for the overall reaction. To complete the minimal reaction scheme, we also measured the elementary rate constants for association and dissociation of tRNA^{Gln} from GluRSND (Figs. 1b and 3). To measure k_{on}, we monitored changes in the intrinsic Trp fluorescence of GluRSND upon addition of tRNA^{Gln}, in the absence of Glu and ATP.[36] Other filter-binding experiments suggest that K_d is not significantly affected by the presence of glutamate and ATP (data not shown). Rate constants obtained from time traces were plotted against tRNA^{Gln} concentration to obtain k_{on} of 1.2×10^8 M^{-1}sec^{-1}. This rate constant is close to the diffusion limit, as expected for tight substrate binding. We then calculated k_{off} of 5.2 sec^{-1} from k_{on} and K_d values, because a direct estimate of k_{off} from the plot of k_{obs} *versus* enzyme concentration is subject to error (Figs. 1b and 3b). This approximation is justified, because the equilibrium constant, $K_{1/2}$ obtained from single-turnover kinetics (Fig. 2c) is equivalent to K_m obtained in steady-state reactions, and is also comparable to K_d measured independently.[31,35] The absence of evidence for lag kinetics in any of the reaction progress curves (Fig. 2b) further suggests that $K_{1/2}$ of 43 ± 18 nM indeed represents K_d.

Binding of GatDE to Glu-tRNA^{Gln} is rate-limiting for k_{cat}/K_m

We next monitored the conversion of Glu-tRNA^{Gln} to Gln-tRNA^{Gln} by GatDE, at saturating ATP and asparagine levels (10 mM and 9.1 mM, respectively; Figs. 4a and b). The Glu-tRNA^{Gln} substrate was obtained from preparative reactions with GluRSND, and then purified for these experiments. Initial velocities monitored under steady state conditions with varying Glu-tRNA^{Gln} concentration yields k_{cat} of 1.47 sec^{-1}, K_m of 4.38 μM, and k_{cat}/K_m of 3.4 × 10^5 M^{-1}sec^{-1}, similar to an earlier report.[37] Under single turnover conditions, saturation of the rate for conversion of Glu-tRNA^{Gln} to Gln-tRNA^{Gln} occurred at about 1 μM GatDE (Figs. 4b and c), giving k_{max} of 1.2 sec^{-1}. This rate was unaffected by inclusion of GluRSND in the reactions at equimolar concentration with GatDE.[31] Because k_{max} is equivalent to k_{cat} obtained in steady-state reactions, it appears that the rate-limiting step is formation of Gln-tRNA^{Gln}, and not its dissociation from GatDE. Consistent with this finding, rates measured under pre-steady state conditions allowing observation of both the first and subsequent turnovers showed no burst of product formation (data not shown). The k_{max} for the GatDE reaction is 10-fold higher than k_{max} for the GluRSND reaction (Fig. 1), implying efficient conversion of Glu-tRNA^{Gln} to Gln-tRNA^{Gln} upon GatDE binding.

To determine the rate-limiting step for the GatDE reaction, we first noted that K_m derived from steady-state measurements is about 10-fold higher than K_d of 690 nM obtained from a filter binding experiment (Fig. S1a). In addition, the rate constant for Glu-tRNA^{Gln} dissociation from GatDE determined from filter binding experiments is about 10-fold lower than the roughly estimated k_{max} of 1.2 sec^{-1} obtained by hand sampling of this fast event (Fig. S1b). These data strongly suggested that binding could be rate-limiting for k_{cat}/K_m, - a case of Briggs-Haldane kinetics in which almost every Glu-tRNA^{Gln} binding event results in Gln-tRNA^{Gln} formation, since substrate dissociation is slow relative to Gln-tRNA^{Gln} formation (Fig. 1b). We therefore directly measured the rate constant for association by using 5′-2-aminopurine labeled Glu-tRNA^{Gln}, which shows fluorescence enhancement upon binding of GatDE (Fig. S2). At 2.5 μM GatDE, the fluorescence change fit well to a single exponential function with a rate constant of 0.64 sec^{-1} (Fig. 4d). The second order rate constant for binding, 2.6 ± 0.1 × 10^5 M^{-1}sec^{-1}, is identical within error to the value of k_{cat}/K_m, and k_{off} calculated from K_d and this k_{on} measurement is also equivalent to the experimental measurement (Fig. S1) – validating this estimate of 1.2 sec^{-1} for dissociation. Thus, association of Glu-tRNA^{Gln} is rate-determining for k_{cat}/K_m in the GatDE-mediated formation of Gln-tRNA^{Gln}.

Two-step dissociative mechanism

The steady-state and elementary rate constants for the separate GluRSND and GatDE reactions (Fig. 1b) allow prediction of reaction progress curve profiles by kinetic modeling, for two scenarios: (i) strict channeling of Glu-tRNA^{Gln} between GluRSND and GatDE in a "transamidosome" complex as previously proposed;[31] (ii) a distributive two-step pathway in which Glu-tRNA^{Gln} is released from GluRSND into solution before binding to GatDE. In the first model, where Gln-tRNA^{Gln} is only formed by channeling (Figs. S3a, S4), free Glu-tRNA^{Gln} does not associate with this particle and is converted to product only in the presence of complexed GatDE. Because k_{max} for GatDE is 10-fold faster than for GluRSND (Fig. 1b), direct channeling implies that Gln-tRNA^{Gln} formation is primarily limited by formation of Glu-tRNA^{Gln}. With fast transfer of Glu-tRNA^{Gln} between GluRSND and GatDE, a channeling model predicts rapid Gln-tRNA^{Gln} formation, without a time lag and with no accumulation of Glu-tRNA^{Gln}.[34] In contrast, a two-step sequential model (Figs. S3b, S5a) predicts that Gln-tRNA^{Gln} formation is limited at least in part by the binding of Glu-tRNA^{Gln} to GatDE. This would result in accumulation of Glu-tRNA^{Gln} in amounts decreasing with increasing concentration of GatDE. A lag in Gln-tRNA^{Gln} formation is also predicted, even at high concentrations of GatDE. Finally, we also model the consequences

of "relaxed" or partial channeling, in which only specified fractions of the Glu-tRNA^{Gln} formed in the first reaction are channeled (Figs. S5b–S5f).

The two limiting kinetic models make distinct predictions regarding formation and reaction of the Glu-tRNA^{Gln} intermediate. To test these models experimentally, we measured Gln-tRNA^{Gln} formation in complete reactions containing both enzymes, tRNA^{Gln}, 10 mM ATP, 50 mM glutamate, and 9.1 mM asparagine as amide donor (Fig. 5). The data shows transient accumulation of Glu-tRNA^{Gln} at all concentrations of GatDE tested, from 10 nM to 6 μM, in the presence of saturating concentration of 600 nM GluRSND (Figs. 5c–5f). The amplitude of Glu-tRNA^{Gln} formation is inversely proportional to the GatDE concentration, as predicted in a distributive model. Lags in the formation of Gln-tRNA^{Gln} were also observed, with durations varying inversely with GatDE concentration. Comparison of the experimental product formation data with the kinetic models demonstrates that the data are consistent only with a two-step mechanism in which Glu-tRNA^{Gln} must dissociate and rebind to GatDE (Figs. 5c–5f). In contrast, models invoking strict or partial channeling made predictions in sharp disagreement with the observed data (Figs. S4 and S5). Since all of the parameters (unimolecular and bimolecular rate constants) were fixed in the kinetic modeling, this high level of correlation between the observed data and our model indicates credibility of the two-step model. Even at 30 μM GatDE, persistent accumulation of about 10% Glu-tRNA^{Gln} is observed (data not shown), as predicted by the dissociative kinetic model at and beyond 30 μM GatDE. Thus, the dissociative model predominates at least up to 30 μM GatDE. From the partial channeling kinetic models, we estimate that at least 80–90% of the Glu-tRNA^{Gln} must dissociate and then rebind to GatDE.

Although the lack of substrate channeling does not exclude formation of a GluRSND-GatDE complex, this finding does call the biological rationale for the proposed "transamidosome" into question. Therefore, although GluRSND-GatDE complex formation was previously investigated by several techniques,[31] we reexamined this question using enzyme preparations produced in our laboratory. Using the identical expression construct and general purification procedure for cleavage and purification of the intein-ligated GluRSND enzyme, we found that exhaustive wash steps after chitin column loading and the use of fresh DTT for intein mediated cleavage, are required to remove a persisting 17 kD contaminant (Fig. S6 and Supplemental Methods). Examination of GluRSND-GatDE complex formation by native gel electrophoresis on both agarose and polyacrylamide gels revealed that only contaminated GluRSND preparations bind to GatDE; further, the isolated contaminant fractions are shown to possess the GatDE binding activity (Fig. S6). Gel filtration HPLC coupled to static light scattering, using the highly purified GluRSND fraction at concentrations in the 10 μM range, similarly failed to reveal formation of GatDE-GluRSND binary complexes. Because evidence of GluRSND homogeneity was not presented in the earlier report, it is not possible to be definitive with respect to the origin of the discrepancy.[31] However, based on our findings with the same expression construct, it is reasonable to suggest that the previously observed formation of a *M. thermautotrophicus* GatDE-GluRSND complex also is due to the contaminating protein, and that a GluRSND-GatDE complex does not form.

Archaeal EF-1α discriminates against Glu-tRNA^{Gln}

Because our findings contradict both binary complex ("transamidosome") formation and the previous proposal for direct channeling of Glu-tRNA^{Gln},[31] we considered alternative mechanisms that might exist in Archaea to avoid misincorporation of Glu at glutamine codons. It is known that the bacterial elongation factor EF-Tu is able to strongly discriminate against Glu-tRNA^{Gln}.[38,39] Archaeal EF-1α proteins are 35% identical in sequence with bacterial EF-Tu (Fig. S7), suggesting that a similar mechanism may function in Archaea. We cloned EF-1α from *M. thermautotrophicus* genomic DNA, purified the

$(His)_6$-affinity-tagged protein to homogeneity, and measured binding to Gln-tRNA^{Gln}, Glu-tRNA^{Glu} and misacylated Glu-tRNA^{Gln} by protection of these species from spontaneous deacylation. In the absence of EF-1α, the rate constant for deacylation is very similar for all three aminoacyl-tRNAs, as expected (Fig. 6). In the presence of 2.2 μM activated EF-1α, there is 24-fold protection of Gln-tRNA^{Gln} and 8-fold protection of Glu-tRNA^{Glu}. In contrast, Glu-tRNA^{Gln} was poorly protected from deacylation at the same concentration of EF-1α, suggesting weaker binding.

To provide a quantitative estimate of the difference in EF-1α binding affinity to misacylated Glu-tRNA^{Gln} *versus* cognate Gln-tRNA^{Gln}, we measured the rate constant for deacylation at varying concentrations of EF-1α (Fig. 7). Gln-tRNA^{Gln} showed both increased protection and a substantial decrease in the rate constant for deacylation with increased levels of EF-1α, allowing derivation of $K_{1/2}$, which is analogous to the binding affinity ($K_{1/2}$ of 0.29 ± 0.03 μM). No protection of Glu-tRNA^{Gln} even at an activated EF-1α concentration of 4.4 μM was observed; from these data, we deduce that Glu-tRNA^{Gln} binds at least 40-fold weaker than Gln-tRNA^{Gln}. The discrimination may arise because EF-1α binds Gln-tRNA^{Gln} with a faster association rate, a slower dissociation rate, or both, compared with its capacity to bind Glu-tRNA^{Gln}.

Further selectivity against incorporation of glutamate at glutamine codons arises from ATP hydrolysis by GatDE, which provides a strongly favorable thermodynamic driving force in the direction of Gln-tRNA^{Gln} formation. At a kinetic level, GatDE and EF-1α function independently, since inclusion of EF-1α at equimolar concentrations in GatDE single-turnover reactions and in combined GluRSND-GatDE reactions is without effect on k_{obs} (data not shown). However, these reactions are thermodynamically coupled, so that selective EF-1α binding of Gln-tRNA^{Gln} will clearly provide a further driving force shifting the equilibrium on GatDE toward product formation. The intracellular level of EF-Tu in bacteria is 100 μM;[56] comparably high concentrations of EF-1α in *M. thermautotrophicus*, if present, would strongly favor this mechanism. We suggest that these considerations are sufficient to account for specificity in glutamine incorporation exceeding the estimated error rate of 10^{-4} in protein synthesis,[40] without the need to invoke either channeling or "transamidosome" formation. Of course, additional capacity for discrimination against noncognate Glu-tRNA^{Gln} may also be available during decoding or post-peptidyl transfer on the ribosome.[41,42]

All canonical, monomeric class I aaRS so far studied exhibit burst kinetics, while the absence of a burst is instead characteristic of class II aaRS.[43] In several class I bacterial aaRS, aminoacylation rates are also enhanced by EF-Tu binding, and observed ternary complexes composed of both proteins with aminoacylated tRNA are consistent with the notion of direct transfer of aminoacylated tRNA. In contrast, class II aaRS are not stimulated by EF-Tu.[43] To test whether the archaeal EF-1α influences the reaction of a nondiscriminating aaRS catalyzing misacylated tRNA formation, we examined its influence on GluRSND kinetics under both steady-state and single-turnover conditions. We found that the inclusion of EF-1α in excess of GluRSND concentration had no effect on the rate of reaction in either case (data not shown). Thus, the previously observed correlation of elongation factor rate enhancement with slow product release in aaRS is maintained. M. *thermautotrophicus* GluRSND remains unusual, however, as it represents a rare example of a class I aaRS that is not rate-limited by the release of aminoacylated tRNA (Fig. 2), thus violating the class-specific rule.[43] The only other known exception is the dimeric tyrosyl-tRNA synthetase.[58]

Discussion

We have applied a general methodology based on pre-steady state kinetics to probe substrate channeling in an RNA-based system, following the approach developed to study channeling in bifunctional metabolic enzymes.[33,34] Previous experimental and computer modeling studies of the GluRS[ND]-GatDE pathway concluded that a protein-protein complex forms between GluRS[ND] and GatDE, and that its formation is essential to sequestering Glu-tRNA[Gln] via a channeling mechanism.[30,31] The pre-steady state kinetic data presented here refutes these notions by demonstrating that the two enzymes function independently: the Glu-tRNA[Gln] intermediate dissociates from GluRS[ND] prior to rebinding GatDE (Figs. 5, 8, S3–S5). We also demonstrate that the GluRS[ND]-GatDE binary complex previously reported may depend on the presence of a contaminating protein, which artefactually binds GatDE (Fig. S6). We cannot detect formation of a protein-protein complex when highly purified materials are used at concentrations up to 10 μM. Clearly, the independent, distributive function of GluRS[ND] and GatDE (Fig. 8) is consistent with the absence of a binary complex.

The lack of influence of either GluRS[ND] or GatDE on the independent reaction of the partner enzyme was noticed previously,[31] but the notion an archaeal-specific transamidosome that functions to sequester Glu-tRNA[Gln] was nonetheless promulgated. Such a binary transamidosome confined to the protein-protein complex alone had been distinguished from proposed bacterial transamidosomes consisting of ternary GatCAB/GluRS[ND]/tRNA[Gln] or GatCAB/AspRS[ND]/tRNA[Asn] complexes,[28–30] where individual enzyme activities are improved upon complex formation, and where channeling was also postulated. The existence of GatCAB-based transamidosomes is clearly well-founded based on the detection of ternary complexes in crystals and in solution. However, the kinetic analyses of the GatCAB systems did not explicitly monitor the misacylated tRNA intermediates and so do not provide evidence for channeling.[28–30] Channeling is certainly plausible in each case, perhaps especially so for the bacterial AspRS[ND]-GatCAB pathway where complex formation strongly stimulates individual enzyme activities.[28] However, a clear demonstration requires transient kinetic measurements. Channeling was also proposed for the two-step pathway to Cys-tRNA[Cys] formation in methanogens,[44] in which phosphoseryl-tRNA synthetase (SepRS) synthesizes a phosphoseryl-tRNA[Cys] misacylated intermediate that is then converted to Cys-tRNA[Cys] by the subsequent enzyme SepCysS. In this case as well, however, a definitive analysis is lacking.[45]

Our results demonstrate that substrate channeling is not required for efficient and precise coding in two-step aminoacylation pathways. The robust mechanisms to prevent misincorporation without channeling in this case include unidirectional conversion of the misacylated intermediate in the ATP-driven GatDE reaction, and at least 40-fold discrimination against Glu-tRNA[Gln] by EF-1α (Fig. 1b and 8). An interesting feature of the pathway is the relatively slow and rate-limiting binding of the misacylated tRNA intermediate by GatDE. While this may appear inefficient, it is known that slow, rate-limiting binding can improve specificity by discriminating against noncognate substrates using a kinetic induced-fit mechanism.[46] Moreover, the finding that GatDE follows Briggs-Haldane kinetics demonstrates an efficient mechanism that precludes dissociation of misacylated tRNA once bound (Fig. 4). Selectivity for Glu-tRNA[Gln] is achieved by close monitoring of the tRNA D-loop by the GatDE tail domain, precluding a productive interaction with the larger D-loop of tRNA[Glu].[27] We speculate that tRNA[Glu] may be rejected by GatDE at the level of complex formation because of slow association or induced-fit, or because it may readily dissociate upon binding. Further detailed kinetic measurements will be required to address these hypotheses.

It is difficult to be definitive in extrapolating these *in vitro* data to the *in vivo* environment of the archaeal cell, because the concentrations of the relevant proteins have not been directly measured. However, in *Escherichia coli* cells, the concentration of each tRNA synthetase is approximately 1 μM,[47] and the levels of individual tRNA isoacceptor families are in the range 2.5 – 10 μM.[48] The experimentally derived estimate of tRNA synthetase concentrations made in *E. coli* is consistent with the levels of prolyl-tRNA synthetase that could be purified from native *Methanocaldococcus jannaschii* cells,[49] suggesting that the abundance of these enzymes may be roughly equivalent in Bacteria and Archaea. If levels of GluRS[ND], GatDE, and tRNA[Gln] in *M. thermautotrophicus* cells are in these ranges, then *in vivo* channeling of Glu-tRNA[Gln] is unlikely since our findings indicate little to no channeling at GatDE concentrations up to 30 μM. Further, we note that in the mammalian cytoplasm where channeling has been demonstrated *in vivo*, the supramolecular architecture of the translation system depends on actin filaments.[50] In Archaea, actin homologs have been found in some Crenarchaeotes and in the Korachaeota,[51] but not among the methanogens, which belong to the Euryarchaeota. An analog to actin (MreB) that performs a cytoskeletal role is found in Bacteria,[52] but no *in vivo* experiments to examine channeling in bacterial translation have been reported. Thus, the popular notion that channeling is prevalent in the early steps of translation in Bacteria and Archaea still lacks a strong experimental foundation. In this regard, direct monitoring of proposed channeled intermediates by transient kinetics, as we have demonstrated here, offers the most definitive available *in vitro* test for comparison with *in vivo* findings.

Materials and Methods

Overexpression and purification of GluRS[ND] and GatDE

The purification of *M. thermautotrophicus* GluRS[ND] followed the general procedure previously reported.[24,25,31,35] pLysS Rosetta cells were grown at 37°C to A_{600} of 0.8, induced with 0.5 mM IPTG, and allowed to grow overnight at 25°C. The cells from 1 liter of saturated culture were centrifuged and resuspended in 35 mL of lysis buffer containing 20 mM sodium Hepes (pH 8.5) and 500 mM NaCl, followed by addition of 150 μg DNAse I, 50 mg lysozyme, and 1 pellet protease inhibitor (Complete Mini, EDTA-free protease inhibitor cocktail tablets – Roche Diagnostics, GmbH, Germany). The cells were sonicated for 5 min with an alternating 2 sec pulse on and pulse off mode using a Branson 450 digital sonicator (Danbury, CT). The cell-free lysate was then centrifuged at 15,000 × rpm for 45 min and the supernatant applied to a 5–10 ml. Chitin affinity matrix (New England Biolabs) pre-equilibrated in lysis buffer. To obtain highly purified enzyme (Fig. S6), the column was washed extensively with five or more column volumes of lysis buffer. The column was then quickly flushed with cleavage buffer containing 500 mM NaCl and 50 mM DTT, using freshly made DTT stock solutions, and the resin then incubated for 8–12 hours to allow cleavage of chitin bound CBP-intein from GluRS[ND]. Cleaved enzyme was then eluted with addition of more cleavage buffer. The recovered material was dialyzed against and stored in a buffer containing 25 mM HEPES-KOH (pH 7.2), 500 mM NaCl, 1 mM DTT, and 50% glycerol. Yield of purified enzyme from one liter of cell culture is about 2 mg. The purity is estimated to be greater than 95% (Fig. S6). See Supplemental Material for further details.

The pET20b-MtGatDE vector for GatDE expression was transformed into pLysS Rosetta cells, and His$_6$-tagged-GatDE was purified as described previously[25]. The cells were grown at 37°C to OD_{600} of 0.8, induced with 0.5 mM IPTG at 15°C and allowed to grow overnight. Two-liter overnight cultures were pooled, centrifuged and cell pellets were resuspended in 25 mL lysis buffer containing 50 mM sodium phosphate (pH 8.0), 300 mM NaCl, and 10 mM imidazole. 150 μg of DNase I, 50 mg of lysozyme, and 1 pellet of protease inhibitor (Complete Mini, EDTA-free protease inhibitor cocktail tablets, Roche Diagnostics, GmbH) were then added. The cell mixture was sonicated for 5 min at an alternating 2 sec pulse on

and pulse off mode using a Branson (Danbury, CT) 450 digital sonicator. The cell-free lysate was then centrifuged at 15000 rpm for 45 min and the supernatant applied to a pre-equilibrated Ni-NTA His-bind resin (Qiagen) column. The column was washed with a buffer containing 50 mM sodium phosphate (pH 8.0), 300 mM NaCl and 20 mM imidazole. The protein was eluted in 50 mM sodium phosphate (pH 8.0), 300 mM NaCl and 250 mM imidazole and dialyzed against 25 mM Hepes-KOH (pH 7.2), 5 mM β-mercaptoethanol, 0.2 mM EDTA, and 50% glycerol. The yield of purified enzyme from 1 L of cell culture is approximately 2 mg. The purity is over 95% as estimated by SDS–PAGE.

In vitro synthesis of tRNA^{Gln} and tRNA^{Glu} transcripts

M. thermautotrophicus tRNA$_2^{Gln}$,[27] and tRNA^{Glu} were prepared by *in vitro* transcription as described previously.[35] DNA templates for tRNA^{Glu} were synthesized from complementary oligodeoxynucleotides with an overlap region. The forward and reverse oligonucleotides used are:
AATTCCTGCAG*TAATACGACTCACTATA*GCTCCGGTAGTGTAGTCCGGCCAATCATTT and:
mUmGGTGCTCCGGCCGGGATTTGAACCCGAGTCTTCGGCTCGAAAGGCCGAAATGATTGG. The underlined sequence represents the T7 promoter. For synthesis of both tRNA^{Glu} and tRNA^{Gln}, 5 mL transcription reactions were performed by incubating 5 μg/mL DNA template, 40 mM DTT, 1mM of each of the four NTPs, 400 mM Tris (pH 8.0), 250 mM MgCl$_2^{2+}$, 20 μM spermidine, 0.1% Triton x-100 and 120 μg/mL Del(172–173) variant of T7 RNA polymerase,[57] for 4 hr at 37°C.[35] The reaction was stopped by adding 0.5 mL of 0.5 mM EDTA; the tRNA was then ethanol precipitated and resuspended in 1 mL water. 40 μL of DNAse was added and the solution incubated for 1 hour at 37°C. The transcript was purified on a 5 mL DEAE column (DE-52; Whatman). The transcript was eluted, ethanol precipitated, resuspended in a buffer containing 10 mM Tris (pH 8.0), 1 mM EDTA (TE), and stored at −20 °C.

3′-labeling of tRNA with α-[^{32}P] ATP

1–2 μM of tRNA^{Gln} or tRNA^{Glu} stored in TE buffer was heated to 80°C in the absence of Mg^{2+}, MgCl$_2$ solution at 80°C was added to a final concentration of 6.25 mM, and the RNA allowed to slow-cool to room temperature. Labeling was performed using tRNA nucleotidyltransferase in the presence of α-[^{32}P] ATP as described previously.[32, 53, 54]

Aminoacylation and amidotransferase kinetics

All reactions were performed in 100 mM HEPES (pH 7.0), 10 mM MgCl$_2^{2+}$ and 5 mM DTT unless otherwise specified. Fast reactions were measured using a Kintek RQF3 rapid chemical quench instrument. All reactions were quenched for 8–10 min in either 400 mM sodium acetate (pH 5.2) containing 0.01 mg/mL P1 nuclease (Fluka), or in 0.1% SDS followed by addition of P1 nuclease to 0.1 mg/mL. Aliquots were spotted on pre-washed PEI-cellulose TLC plates (Sigma) and developed in a solution containing 100 mM ammonium acetate, 5% (v/v) acetic acid. The plates were dried and quantitated by phosphorimaging. [^{32}P]-labeled AMP, Gln-AMP and Glu-AMP migrate at clearly distinguishable positions. Quantitation was done with Imagequant (version 5.2) and Kaleidagraph (version 4.03).

Purification of α-[^{32}P] labeled Glu-tRNA^{Gln} and Gln-tRNA^{Gln}

Purified 3′-[^{32}P] labeled Glu-tRNA^{Gln} and Gln-tRNA^{Gln} were obtained by aminoacylation under conditions similar to that described in the previous section, except that the Hepes buffer concentration was reduced to 5 mM to facilitate buffer exchange. The aminoacylation reaction was performed with 100 nM GluRSND alone or with a mixture of 100 nM GluRSND

and 100 nM GatDE for 20 minutes. Immediately following the reaction, the pH was lowered by addition of 100 mM sodium acetate (pH 5.2), and the aminoacylated tRNAs were acid phenol-chloroform extracted and buffer exchanged four times with 10 mM sodium acetate (pH 5.2) and 1 mM EDTA (SE) buffer using Amicon ultra-0.5 filters (Millipore). The aminoacylation levels of [^{32}P]-Glu-tRNA^{Gln} and [^{32}P]-Gln-tRNA^{Gln} were quantitated by complete digestion of the tRNAs with P1 nuclease followed by TLC analysis in the same solvent system used to monitor aminoacylation and amidotransferase timecourses (see above). The aminoacyl-tRNAs were stored in SE buffer at −20°C and used within 2 days.

Fluorescence stopped-flow measurements

Binding of tRNA^{Gln} to GluRSND was monitored by stopped-flow fluorimetry using the intrinsic Trp fluorescence signal, while binding of Glu-tRNA^{Gln} to GatDE utilized 2-aminopurine (2AP) attached to the tRNA 5′-end. For 5′-2AP labeling, tRNA^{Gln} was misacylated by GluRSND to form Glu-tRNA^{Gln} at levels corresponding to 60% of the RNA, and this product purified by acid phenol-chloroform extraction and exchange into SE buffer (see section above on purification of α-[^{32}P] labeled aminoacyl-tRNAs). Aminoacylation protects the 3′end of the tRNA in the 5′-labeling reaction. For labeling, Glu-tRNA^{Gln} was incubated with 1 mM 2-AP triphosphate (Biolog lifescience, Germany), 10 mM MgCl$_2$, 50 mM Hepes (pH 7.0) and 10 U/μL T4 ligase I at 37°C for 5 min.[55] This was followed immediately by addition of sodium acetate (pH 5.2) to a final concentration of 167 mM, and purification by acid-phenol chloroform extraction and exchange into SE buffer. 2AP-labeled Glu-tRNA^{Gln} is stored at −20°C and used within 2 days.

Rapid binding kinetics were measured using a stopped-flow fluorescence instrument (Applied Photophysics SX.18MV). For GluRSND, the change in intrinsic Trp fluorescence was monitored upon binding of tRNA^{Gln}. The excitation wavelength was 285 nm and emission was monitored through a 305 nm cut-off filter. Experiments were initiated by mixing tRNA from one syringe with enzyme from the second syringe. Fluorescence traces were fit to the equation:

$$F=(F_{max} - F_0)(e^{-kobs*t})+F_0 \tag{1}$$

where F is fluorescence in arbitrary units, F_{max} is maximum fluorescence amplitude, F_0 is the initial fluorescence, k_{obs} is the rate constant in units of sec^{-1}, and t is time in units of seconds. A control experiment in which enzyme was mixed with buffer alone, rather than tRNA, gave no change in the fluorescence.

At least four traces were obtained for every concentration of tRNA^{Gln} and the average k_{obs} is reported. k_{on} and k_{off} were obtained by fitting to the equation:[36]

$$k_{obs}=k_{on}[tRNA^{Gln}]+k_{off} \tag{2}$$

The binding of Glu-tRNA^{Gln} to GatDE was monitored with 5′ 2-AP labeled substrate. The excitation wavelength used was 307 nm, and increase in the fluorescence of 2-AP Glu-tRNA^{Gln} upon rapid mixing with GatDE was monitored through a 320 nm cut-off filter. Three traces were averaged to obtain k_{obs}. k_{obs} was divided by the concentration of GatDE used, 2.5 μM, to derive the k_{on} value. Fluorescence traces were fit to the equation:

$$F=(F_{max} - F_0)(1 - e^{-kobs*t})+F_0 \tag{3}$$

EF-1α protection assay

EF-1α was cloned, overexpressed, and purified as described in the Supplementary Material. The purified EF-1α was activated (see below) prior to performing protection assays. To perform protection assays, purified $[^{32}P]$Gln-tRNA^{Gln}, $[^{32}P]$Glu-tRNA^{Gln} or $[^{32}P]$Glu-tRNA^{Glu} were added to a 20μL reaction containing activated EF-1α or a buffer control, in the presence of 100 mM Hepes (pH 7.0), 10 mM MgCl$_2$, 5 mM DTT, 6 mM phosphoenol pyruvate, 6 μg/mL pyruvate kinase, 100 mM ammonium chloride, and 2 mM MgCl$_2$. The fraction of deacylated tRNA at 37°C over time was measured by quenching 3 μL aliquots from the 20 μL reaction in 15 μl quench solution containing 5 μl of 400 mM sodium acetate (pH 5.2) and 10 μl phenol-chloroform. After vigorous mixing, the tRNA was extracted, and P1 nuclease was added at 75 μg/ml to the recovered tRNA, followed by separation of substrate and products by TLC as described above. Rate constants for protection of deacylation, as a function of EF-1α concentration, were fit to the following equation:[59]

$$k_{obs} = \frac{(k_{unprotected})}{1 + ([EF - 1\alpha]/K_{1/2})}$$

(4)

where $k_{unprotected}$ is the observed rate constant for deacylation in the absence of EF-1α, and $K_{1/2}$ is the affinity of EF-1α to Gln-tRNA^{Gln}.

EF-1α activation

EF-1α was activated by incubating in 100 mM Hepes (pH 7.0), 10 mM MgCl$_2$, 5 mM DTT, 6 mM phosphoenol pyruvate, 6 μg/mL pyruvate kinase, 100 mM ammonium chloride, and 2 mM Mg^{2+}-GTP at 37°C for over 24 hours. The fraction of active EF-1α was determined by incubating 50 μM EF-1α with different concentrations of $[^{32}P]$-α labeled GTP. The mixture was then filtered through a nitrocellulose membrane. The membranes were immediately washed with 100 mM Hepes (pH 7.0), 10 mM MgCl$_2$, 5 mM DTT wash buffer, dried, and subject to phosphorimaging analysis. The amount of GTP bound by EF-1α reflects the fraction of EF-1α that is active. At different concentrations of GTP and EF-1α, the same fraction was active, i.e., about 8.85%, and the term "activated" EF-1α reflects this correction.

Kinetic simulations

All simulations were performed using Berkeley Madonna, Ver 8.3.14 (Macey and Oster, UC-Berkeley) by Runge-Kutta 4 integration method. The chemical reaction module of Madonna was used for constructing initial models. The reactant and product concentrations as shown for each model in Figure 3 were directly input in the "Reactants" and "Products" boxes. Both forward and reverse rate constants at each step were assigned. Reverse rate constants for catalytic steps (tRNA aminoacylation and ATP-dependent amidotransferase) were presumed to be very slow and were assigned values of zero. First-order and second-order rate constants were directly input keeping the same units for consistency (sec^{-1} for 1st order and M^{-1}sec^{-1} for 2nd order). Initial GatDE concentration was input at 600 nM, but was varied using the Define slider option to 0 nM, 10 nM, 100 nM, 600 nM and 6 μM. GluRSND and tRNA concentrations were fixed at 600 nM and 100 pM, respectively; varying the concentration of tRNA did not affect the simulated plot as long as the tRNA concentration was maintained below the enzyme concentration. All parameters (first and second order rate constants) were fixed and not allowed to change. For the two step dissociative mechanism (Figure S4b), the fraction of Glu-tRNA^{Gln} and Gln-tRNA^{Gln} were defined in the equations window as Fraction P = P+E2P/(S+ES+P+E2P+E2P2+P2) and Fraction P2 = P2/(S+ES+EP+P+E2P+E2P2+P2), where S, ES, P, E2P, P2 and E2P2

represent tRNA^{Gln}, GluRSND:tRNA^{Gln}, Glu-tRNA^{Gln}, GatDE:Glu-tRNA^{Gln}, Gln-tRNA^{Gln} and GatDE:Gln-tRNA^{Gln}, respectively. For purposes of simplicity, the product dissociation steps are not shown in Fig. S3. Since product dissociation was found to be faster than reaction for both GluRSND and GatDE (see text), any rate constant greater than 1 sec^{-1} for Glu-tRNA^{Gln} dissociation from GluRSND and greater than 10 sec^{-1} for Gln-tRNA^{Gln} dissociation from GatDE did not affect the simulated plots. We therefore fixed these rate constants at 50 sec^{-1}. The definition of fractions P and P2 were appropriately modified for the channeled and partially channeled pathways.

Estimate of errors

Many experiments were performed with two to three different preparations of GluRSND and/ or GatDE, and consistency was verified. Most experiments were repeated in triplicate, and all reactions were performed at least twice; error estimates are provided as mean ± standard deviation.

Supplementary Material

Refer to Web version on PubMed Central for supplementary material.

Acknowledgments

References

1. Anderson KS. Fundamental mechanisms of substrate channeling. Methods Enzymol. 1999; 308:111–126. [PubMed: 10507003]

2. Huang X, Holden HM, Raushel FM. Channeling of substrates and intermediates in enzyme-catalyzed reactions. Annu Rev Biochem. 2001; 70:149–180. [PubMed: 11395405]

3. An S, Kumar R, Sheets ED, Benkovic SJ. Reversible compartmentalization of de novo purine biosynthetic complexes in living cells. Science. 2008; 320:103–106. [PubMed: 18388293]

4. Lenaz G, Genova ML. Structure and organization of mitochondrial respiratory complexes: a new understanding of an old subject. Antioxid Redox Signal. 2010; 12:961–1008. [PubMed: 19739941]

5. Meyer FM, Gerwig J, Hammer E, Herzberg C, Commichau FM, Volker U, Stulke J. Physical interactions between tricarboxylic acid cycle enzymes in Bacillus subtilis: evidence for a metabolon. Metab Eng. 2011; 13:18–27. [PubMed: 20933603]

6. Kuhner S, van Noort V, Betts MJ, Leo-Macias A, Batisse C, Rode M, Yamada T, Maier T, Bader S, Beltran-Alvarez P, Castano-Diez D, Chen WH, Devos D, Guell M, Norambuena T, Racke I, Rybin V, Schmidt A, Yus E, Aebersold R, Herrmann R, Bottcher B, Frangakis AS, Russell RB, Serrano L, Bork P, Gavin AC. Proteome organization in a genome-reduced bacterium. Science. 2009; 326:1235–1240. [PubMed: 19965468]

7. Tarassov K, Messier V, Landry CR, Radinovic S, Serna Molina MM, Shames I, Malitskaya Y, Vogel J, Bussey H, Michnick SW. An *in vivo* map of the yeast protein interactome. Science. 2008; 320:1465–1470. [PubMed: 18467557]

8. Negrutskii BS, Deutscher MP. Channeling of aminoacyl-tRNA for protein synthesis *in vivo*. Proc Natl Acad Sci U S A. 1991; 88:4991–4995. [PubMed: 2052582]

9. Stapulionis R, Deutscher MP. A channeled tRNA cycle during mammalian protein synthesis. Proc Natl Acad Sci U S A. 1995; 92:7158–7161. [PubMed: 7638160]

10. Kerjan P, Cerini C, Semeriva M, Mirande M. The multienzyme complex containing nine aminoacyl-tRNA synthetases is ubiquitous from Drosophila to mammals. Biochim Biophys Acta. 1994; 1199:293–297. [PubMed: 8161568]

11. Kyriacou SV, Deutscher MP. An important role for the multienzyme aminoacyl-tRNA synthetase complex in mammalian translation and cell growth. Mol Cell. 2008; 29:419–427. [PubMed: 18313381]

12. Hausmann CD, Praetorius-Ibba M, Ibba M. An aminoacyl-tRNA synthetase:elongation factor complex for substrate channeling in archaeal translation. Nucleic Acids Res. 2007; 35:6094–6102. [PubMed: 17766929]

13. Großhans H, Simos G, Hurt E. Review: transport of tRNA out of the nucleus-direct channeling to the ribosome? J Struct Biol. 2000; 129:288–294. [PubMed: 10806079]

14. Brandt F, Carlson LA, Hartl FU, Baumeister W, Grünewald K. The three-dimensional organization of polyribosomes in intact human cells. Mol Cell. 2010; 39:560–569. [PubMed: 20797628]

15. Huber D, Rajagopalan N, Preissler S, Rocco MA, Merz F, Kramer G, Bukau B. SecA interacts with ribosomes in order to facilitate posttranslational translocation in bacteria. Mol Cell. 2011; 41:343–353. [PubMed: 21292166]

16. Godinic-Mikulcic V, Jaric J, Hausmann CD, Ibba M, Weygand-Durasevic I. An archaeal tRNA-synthetase complex that enhances aminoacylation under extreme conditions. J Biol Chem. 2011; 286:3396–3404. [PubMed: 21098026]

17. Hausmann CD, Ibba M. Structural and functional mapping of the archaeal multi-aminoacyl-tRNA synthetase complex. FEBS Lett. 2008; 582:2178–2182. [PubMed: 18538672]

18. Karanasios E, Simader H, Panayotou G, Suck D, Simos G. Molecular determinants of the yeast Arc1p-aminoacyl-tRNA synthetase complex assembly. J Mol Biol. 2007; 374:1077–1090. [PubMed: 17976650]

19. Curnow AW, Ibba M, Söll D. tRNA-dependent asparagine formation. Nature. 1996; 382:589–590. [PubMed: 8757127]

20. Schon A, Kannangara CG, Gough S, Söll D. Protein biosynthesis in organelles requires misaminoacylation of tRNA. Nature. 1988; 331:187–190. [PubMed: 3340166]

21. Wilcox M, Nirenberg M. Transfer RNA as a cofactor coupling amino acid synthesis with that of protein. Proc Natl Acad Sci U S A. 1968; 61:229–236. [PubMed: 4972364]

22. Fersht AR, Kaethner MM. Mechanism of aminoacylation of tRNA. Proof of the aminoacyl adenylate pathway for the isoleucyl- and tyrosyl-tRNA synthetases from Escherichia coli K12. Biochemistry. 1976; 15:818–823. [PubMed: 764868]

23. Curnow AW, Hong K, Yuan R, Kim S, Martins O, Winkler W, Henkin TM, Söll D. Glu-tRNAGln amidotransferase: a novel heterotrimeric enzyme required for correct decoding of glutamine codons during translation. Proc Natl Acad Sci U S A. 1997; 94:11819–11826. [PubMed: 9342321]

24. Tumbula DL, Becker HD, Chang WZ, Söll D. Domain-specific recruitment of amide amino acids for protein synthesis. Nature. 2000; 407:106–110. [PubMed: 10993083]

25. Feng L, Sheppard K, Tumbula-Hansen D, Söll D. Gln-tRNA^{Gln} formation from Glu-tRNA^{Gln} requires cooperation of an asparaginase and a Glu-tRNA^{Gln} kinase. J Biol Chem. 2005; 280:8150–8155. [PubMed: 15611111]

26. Nakamura A, Yao M, Chimnaronk S, Sakai N, Tanaka I. Ammonia channel couples glutaminase with transamidase reactions in GatCAB. Science. 2006; 312:1954–1958. [PubMed: 16809541]

27. Oshikane H, Sheppard K, Fukai S, Nakamura Y, Ishitani R, Numata T, Sherrer RL, Feng L, Schmitt E, Panvert M, Blanquet S, Mechulam Y, Söll D, Nureki O. Structural basis of RNA-dependent recruitment of glutamine to the genetic code. Science. 2006; 312:1950–1954. [PubMed: 16809540]

28. Bailly M, Blaise M, Lorber B, Becker HD, Kern D. The transamidosome: a dynamic ribonucleoprotein particle dedicated to prokaryotic tRNA-dependent asparagine biosynthesis. Mol Cell. 2007; 28:228–239. [PubMed: 17964262]

29. Blaise M, Bailly M, Frechin M, Behrens MA, Fischer F, Oliveira CL, Becker HD, Pedersen JS, Thirup S, Kern D. Crystal structure of a transfer-ribonucleoprotein particle that promotes asparagine formation. Embo J. 2010; 29:3118–3129. [PubMed: 20717102]

30. Ito T, Yokoyama S. Two enzymes bound to one transfer RNA assume alternative conformations for consecutive reactions. Nature. 2010; 467:612–616. [PubMed: 20882017]

31. Rampias T, Sheppard K, Söll D. The archaeal transamidosome for RNA-dependent glutamine biosynthesis. Nucleic Acids Res. 2010; 38:5774–5783. [PubMed: 20457752]

32. Uter NT, Perona JJ. Long-range intramolecular signaling in a tRNA synthetase complex revealed by pre-steady-state kinetics. Proc Natl Acad Sci U S A. 2004; 101:14396–14401. [PubMed: 15452355]

33. Liang PH, Anderson KS. Substrate channeling and domain-domain interactions in bifunctional thymidylate synthase-dihydrofolate reductase. Biochemistry. 1998; 37:12195–12205. [PubMed: 9724533]

34. Bulock KG, Beardsley GP, Anderson KS. The kinetic mechanism of the human bifunctional enzyme ATIC (5-amino-4-imidazolecarboxamide ribonucleotide transformylase/inosine 5′-monophosphate cyclohydrolase). A surprising lack of substrate channeling. J Biol Chem. 2002; 277:22168–22174. [PubMed: 11948179]

35. Rodriguez-Hernandez A, Bhaskaran H, Hadd A, Perona JJ. Synthesis of Glu-tRNA^{Gln} by engineered and natural aminoacyl-tRNA synthetases. Biochemistry. 2010; 49:6727–6736. [PubMed: 20617848]

36. Hong KW, Ibba M, Weygand-Durasevic I, Rogers MJ, Thomann HU, Söll D. Transfer RNA-dependent cognate amino acid recognition by an aminoacyl-tRNA synthetase. Embo J. 1996; 15:1983–1991. [PubMed: 8617245]

37. Sheppard K, Sherrer RL, Söll D. Methanothermobacter thermautotrophicus tRNA^{Gln} confines the amidotransferase GatCAB to asparaginyl-tRNA^{Asn} formation. J Mol Biol. 2008; 377:845–853. [PubMed: 18291416]

38. Asahara H, Uhlenbeck OC. The tRNA specificity of Thermus thermophilus EF-Tu. Proc Natl Acad Sci U S A. 2002; 99:3499–3504. [PubMed: 11891293]

39. LaRiviere FJ, Wolfson AD, Uhlenbeck OC. Uniform binding of aminoacyl-tRNAs to elongation factor Tu by thermodynamic compensation. Science. 2001; 294:165–168. [PubMed: 11588263]

40. Ling J, Reynolds N, Ibba M. Aminoacyl-tRNA synthesis and translational quality control. Annu Rev Microbiol. 2009; 63:61–78. [PubMed: 19379069]

41. Schrader JM, Chapman SJ, Uhlenbeck OC. Tuning the affinity of aminoacyl-tRNA to elongation factor Tu for optimal decoding. Proc Natl Acad Sci U S A. 2011; 108:5215–5220. [PubMed: 21402928]

42. Zaher HS, Green R. Quality control by the ribosome following peptide bond formation. Nature. 2009; 457:161–166. [PubMed: 19092806]

43. Zhang CM, Perona JJ, Ryu K, Francklyn C, Hou YM. Distinct kinetic mechanisms of the two classes of Aminoacyl-tRNA synthetases. J Mol Biol. 2006; 361:300–311. [PubMed: 16843487]

44. Sauerwald A, Zhu W, Major TA, Roy H, Palioura S, Jahn D, Whitman WB, Yates JR 3rd, Ibba M, Söll D. RNA-dependent cysteine biosynthesis in archaea. Science. 2005; 307:1969–1972. [PubMed: 15790858]

45. Zhang CM, Liu C, Slater S, Hou YM. Aminoacylation of tRNA with phosphoserine for synthesis of cysteinyl-tRNA^{Cys}. Nat Struct Mol Biol. 2008; 15:507–514. [PubMed: 18425141]

46. Karbstein K, Herschlag D. Extraordinarily slow binding of guanosine to the Tetrahymena group I ribozyme: implications for RNA preorganization and function. Proc Natl Acad Sci U S A. 2003; 100:2300–2305. [PubMed: 12591943]

47. Jakubowski H, Goldman E. Quantities of individual aminoacyl-tRNA families and their turnover in Escherichia coli. J Bacteriol. 1984; 158:769–776. [PubMed: 6373741]

48. Dong H, Nilsson L, Kurland CG. Co-variation of tRNA abundance and codon usage in Escherichia coli at different growth rates. J Mol Biol. 1996; 260:649–663. [PubMed: 8709146]

49. Lipman RS, Sowers KR, Hou YM. Synthesis of cysteinyl-tRNA(Cys) by a genome that lacks the normal cysteine-tRNA synthetase. Biochemistry. 2000; 39:7792–7798. [PubMed: 10869184]

50. Stapulionis R, Kolli S, Deutscher MP. Efficient mammalian protein synthesis requires an intact F-actin system. J Biol Chem. 1997; 272:24980–24986. [PubMed: 9312103]

51. Ettema TJ, Lindas AC, Bernander R. An actin-based cytoskeleton in archaea. Mol Microbiol. 2011; 80:1052–1061. [PubMed: 21414041]

52. van den Ent F, Amos LA, Lowe J. Prokaryotic origin of the actin cytoskeleton. Nature. 2001; 413:39–44. [PubMed: 11544518]

53. Bullock TL, Uter N, Nissan TA, Perona JJ. Amino acid discrimination by a class I aminoacyl-tRNA synthetase specified by negative determinants. J Mol Biol. 2003; 328:395–408. [PubMed: 12691748]

54. Wolfson AD, Uhlenbeck OC. Modulation of tRNA^{Ala} identity by inorganic pyrophosphatase. Proc Natl Acad Sci U S A. 2002; 99:5965–5970. [PubMed: 11983895]

55. Kinoshita Y, Nishigaki K, Husimi Y. Fluorescence-, isotope- or biotin-labeling of the 5′-end of single-stranded DNA/RNA using T4 RNA ligase. Nucleic Acids Res. 1997; 25:3747–3748. [PubMed: 9278501]

56. Blanquet, S.; Mechulam, Y.; Schmitt, E.; Vial, L. Aminoacyl-transfer RNA maturation. In: Lapointe, J.; Brakier-Gingras, L., editors. Translation Mechanisms. Kluwer Academic/Plenum Publishers; New York, NY: 2003. p. 65-79.

57. Lyakhov DL, He B, Zhang X, Studier FW, Dunn JJ, McAllister WT. Mutant bacteriophage T7 RNA polymerases with altered termination properties. J Mol Biol. 1997; 269:28–40. [PubMed: 9192998]

58. Avis JM, Day AG, Garcia GA, Fersht AR. Reaction of modified and unmodified tRNA^{Tyr} substrates with tyrosyl-tRNA synthetase (*Bacillus stearothermophilus*). Biochemistry. 1993; 32:5312–5320. [PubMed: 8499435]

59. Karbstein K, Doudna JA. GTP-dependent formation of a ribonucleoprotein subcomplex required for ribosome biogenesis. J Mol Biol. 2006; 356:432–443. [PubMed: 16376378]

Highlights

Distributive enzyme function maintains protein quality control in Archaea

Action of elongation factor contributes to stringency of glutamine coding in Archaea

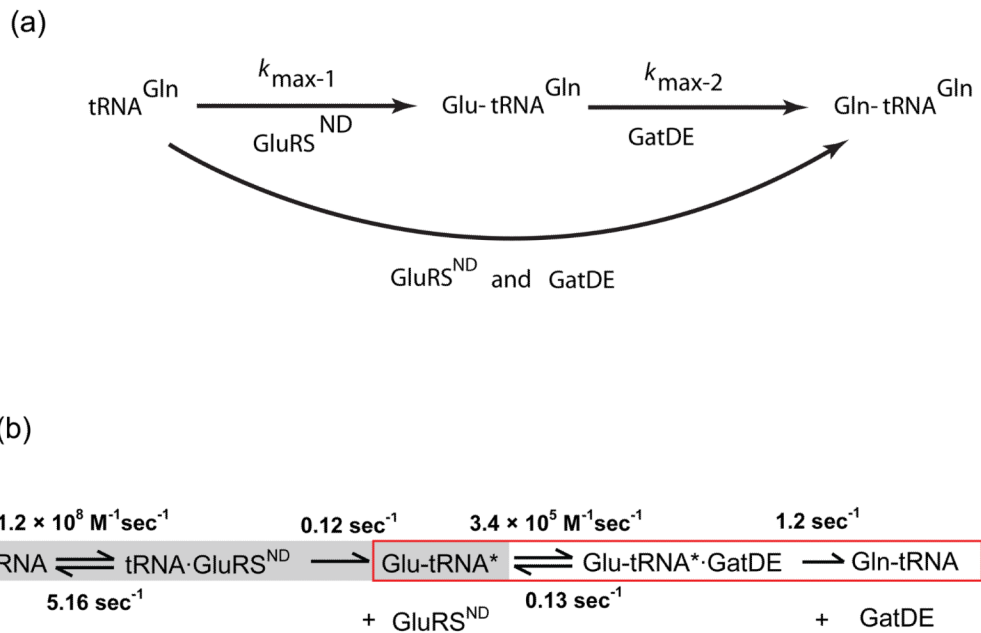Explicit monitoring of metabolic intermediates is required to demonstrate channeling

(a)

(b)

Fig. 1.
Kinetics of the two-step pathway for Gln-tRNA^{Gln} formation in the archaeon *M. thermautotrophicus*. (a) Experimental design used to investigate the possibility that the intermediate Glu-tRNA^{Gln} is channeled from GluRSND to GatDE. (b) Summary of rate constants for individual steps in the two-step pathway for Gln-tRNA^{Gln} synthesis, derived from experiments presented in thjis manuscript.
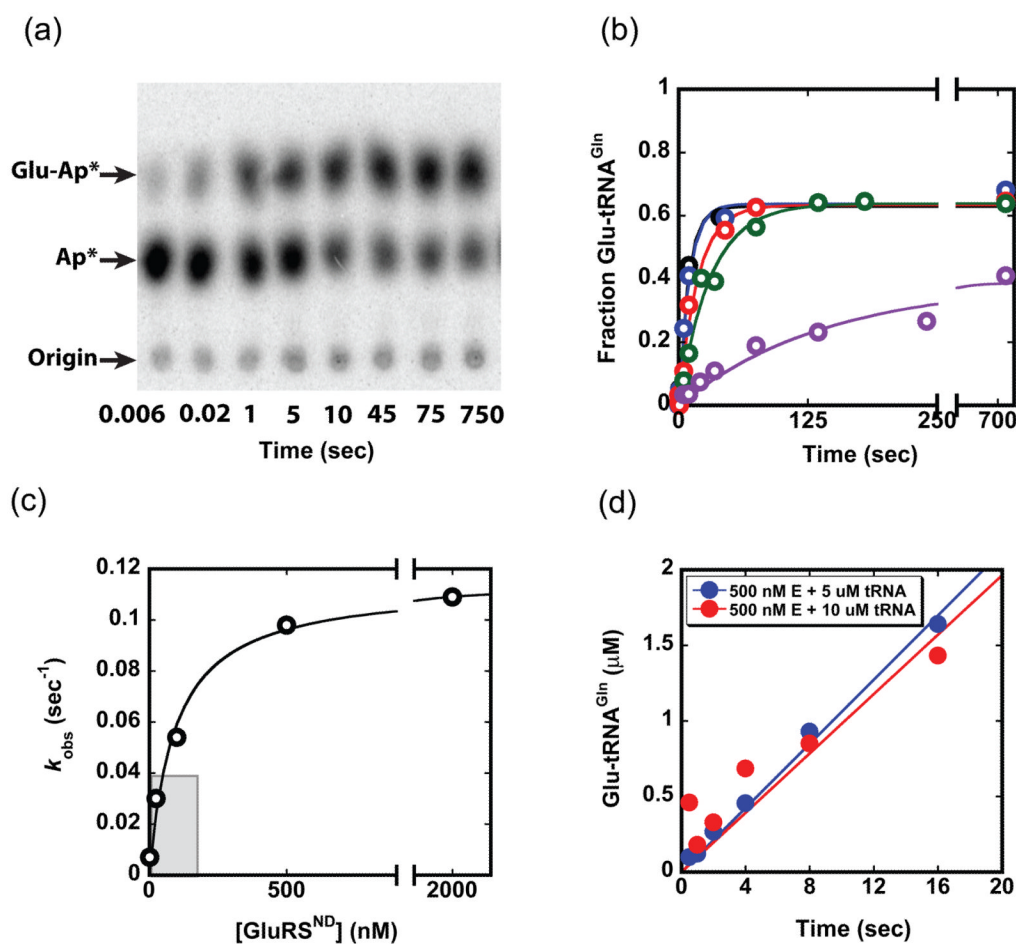
Fig. 2.
Kinetics of the tRNA^{Gln} aminoacylation reaction. (a) Thin-layer chromatography (TLC) separation of substrate and products from a single turnover reaction at 500 nM enzyme (quantitated in b). Plateau aminoacylation levels for the reaction are consistemtly in the 60–70% range. (b) Time traces of product formation at enzyme concentrations of 2 nM (purple), 25 nM (green), 100 nM (red), 500 nM (blue) and 2 μM (black). The tRNA^{Gln} concentration in each reaction is < 1 nM. Curves are fit to $F = F_{max}(1-e^{-kt})$, where F is the fraction Glu-tRNA^{Gln} formed, F_{max} is the maximum (plateau) value of F, k is the rate constant (sec^{-1}) and t is time (sec). (c) Plot of k_{obs} values obtained from the data in panel (b) as a function of GluRSND concentration; from this plot we derive k_{max} of 0.12 ± 0.01 sec^{-1} and $K_{1/2}$ of 43 ± 18 nM. The curve is fit to: $k_{obs} = k_{obs,max}[GluRS^{ND}]/(K_{1/2} + [GluRS^{ND}])$. (d) Pre-steady state kinetic timecourses at 500 nM GluRSND and either 5 μM (blue) or 10 μM tRNA^{Gln} (red).
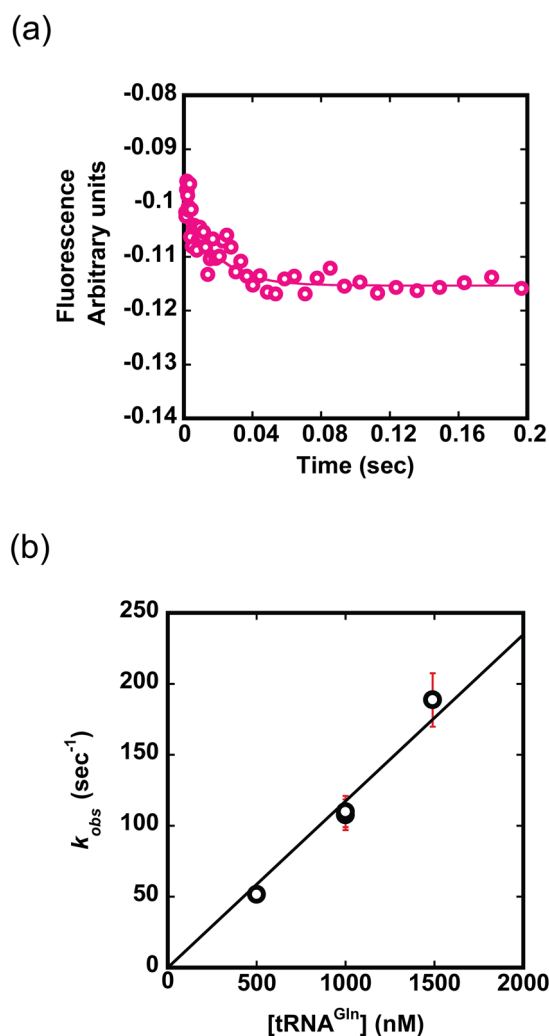
(a)

(b)

Fig. 3.
Binding of tRNA^{Gln} to GluRSND. (a) Time course monitoring the decrease in intrinsic Trp fluorescence upon addition of varying concentrations of tRNA^{Gln} using a stopped-flow instrument. A sample trace at 500 nM GluRSND and 500 nM tRNA^{Gln} is shown, from which k_{obs} of 50 sec^{-1} was derived. (b) Plot of observed association constants against concentration of tRNA^{Gln}, from which k_{on} of 1.2×10^8 M^{-1}sec^{-1} is derived. Equations to fit the raw data and to derive elementary rate constants are provided in Materials and Methods (equations (1) and (2), respectively).

(a)

(b)

(c)

(d)
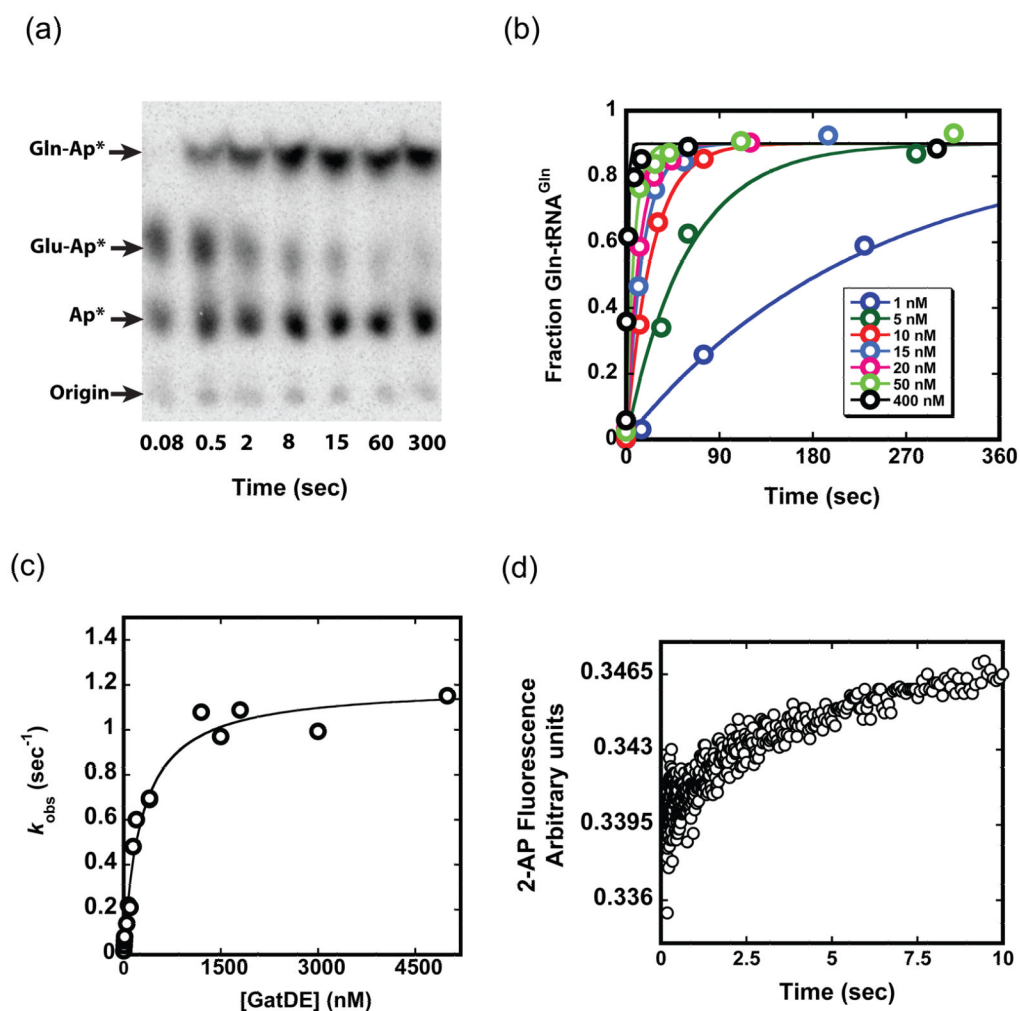
Fig. 4.
Kinetics of the GatDE reaction. (a) Timecourse of a GatDE reaction showing TLC separation of Gln-tRNA^{Gln} from Glu-tRNA^{Gln} and tRNA^{Gln}. (b) Time traces for the formation of Gln-tRNA^{Gln} from purified Glu-tRNA^{Gln} under single turnover conditions. Concentrations are less than 1 nM for Glu-tRNA^{Gln} and as depicted for GatDE. Curves are fit to $F = F_{max}(1-e^{-kt})$, where F is the fraction Gln-tRNA^{Gln} formed, F_{max} is the maximum (plateau) value of F, k is the rate constant (sec^{-1}) and t is time (sec). (c) Plot of the GatDE concentration dependence of k_{obs} obtained from (b); from which we derive k_{max} of 1.2 ± 0.04 sec^{-1}. The curve is fit to: $k_{obs} = k_{obs,max}[GatDE]/(K_{1/2} + [GatDE])$. (d) Increase in fluorescence of 2-AP labeled tRNA (average of three traces) upon binding of 2.5 μM GatDE giving k_{on} of $2.6 \pm 0.11 \times 10^5$ M^{-1}sec^{-1}. The equation used to fit the raw fluorescence data is provided in Materials and Methods (equation 3).
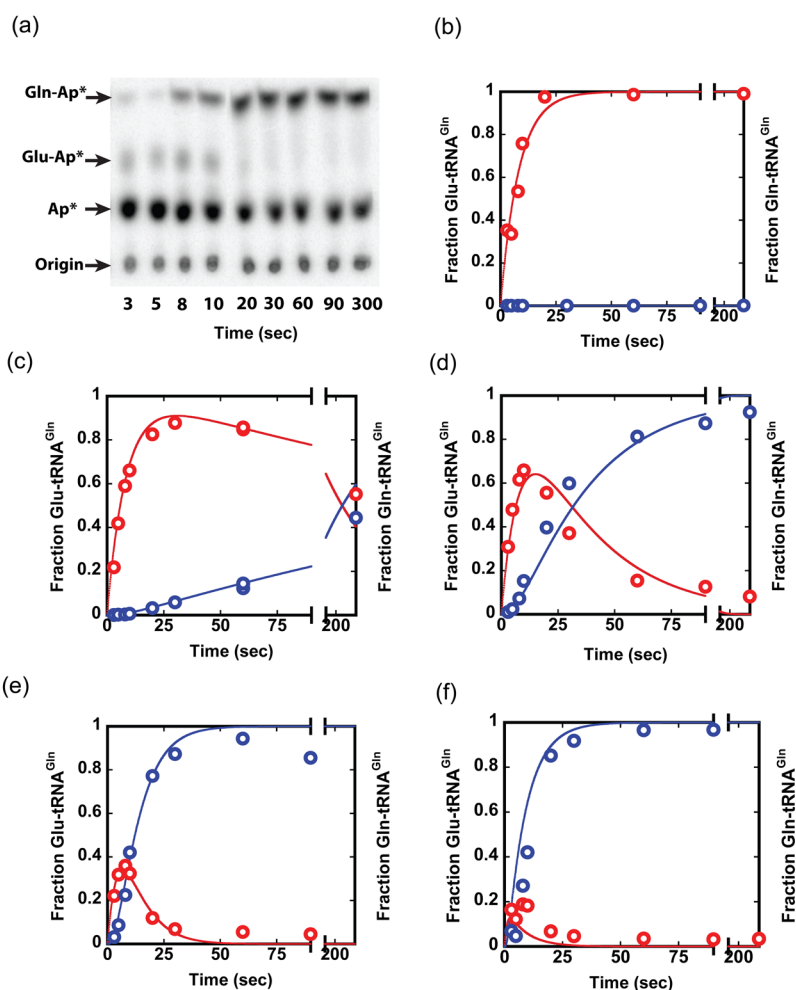
Fig. 5.
Combined GluRS[ND] and GatDE reactions. (a) TLC plate showing transient accumulation of the Glu-tRNA[Gln] intermediate during conversion of tRNA[Gln] to Gln-tRNA[Gln] in the presence of both GluRS[ND] (600 nM) and GatDE (600 nM). Plots of normalized data and kinetic simulation traces (not fits to data) for a two-step dissociative mechanism at 600 nM GluRS[ND] and GatDE at 0 nM (a), 10 nM (b), 100 nM (c), 600 nM (d) and 6 μM (e). tRNA[Gln] in all the reactions < 1 nM. The panels show that, at all tested concentrations of GatDE, a distributive model fits the data well. Goodness of fit values (R^2) from the nonlinear regression were computed separately using GraphPad software; for formation and reaction of Glu-tRNA[Gln] these values range from 0.91 to 0.97. See Supplementary Figs. S3–S5 for details of kinetic simulations and evidence that a channeling model does not fit the data.
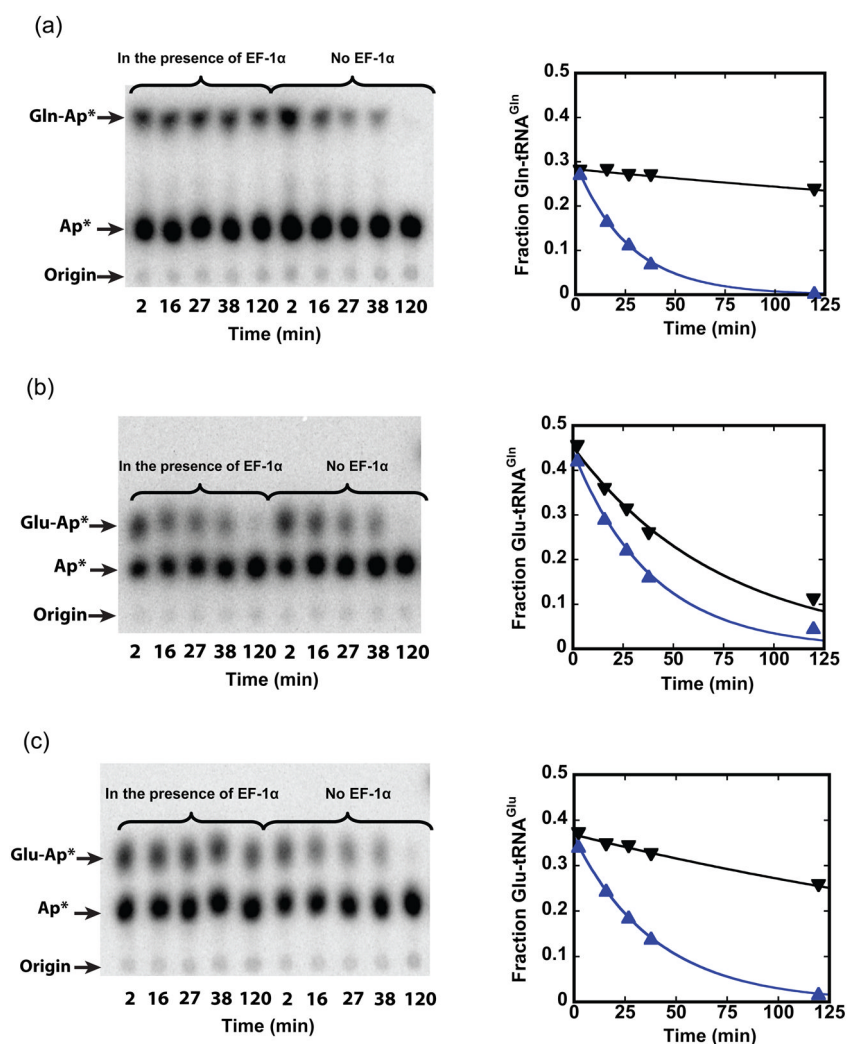
Fig. 6.
Discrimination against Glu-tRNA^{Gln} by archaeal EF-1α. TLC images showing spots corresponding to acylated (Gln-Ap*) and deacylated (Ap*) tRNAs (left panels) were quantified to give the fraction of (a) Gln-tRNA^{Gln}, (b) Glu-tRNA^{Gln} and (c) Glu-tRNA^{Glu} in the presence of 2.2 μM activated EF-1α (inverted triangles) or in the presence of activated EF-1α following proteinase K incubation for 10 minutes (triangles). When EF-1α is removed by proteolysis, the rate constants for spontaneous deacylation are 0.036 min^{-1}, 0.025 min^{-1}, and 0.025 min^{-1} for the three aminoacyl-tRNAs, respectively (blue traces). In the presence of activated EF-1α, the rate constants are: 0.0015 min^{-1} for Gln-tRNA^{Gln}, 0.013 min^{-1} for Glu-tRNA^{Gln}, and 0.003 min^{-1} for Glu-tRNA^{Glu}, respectively (black traces).
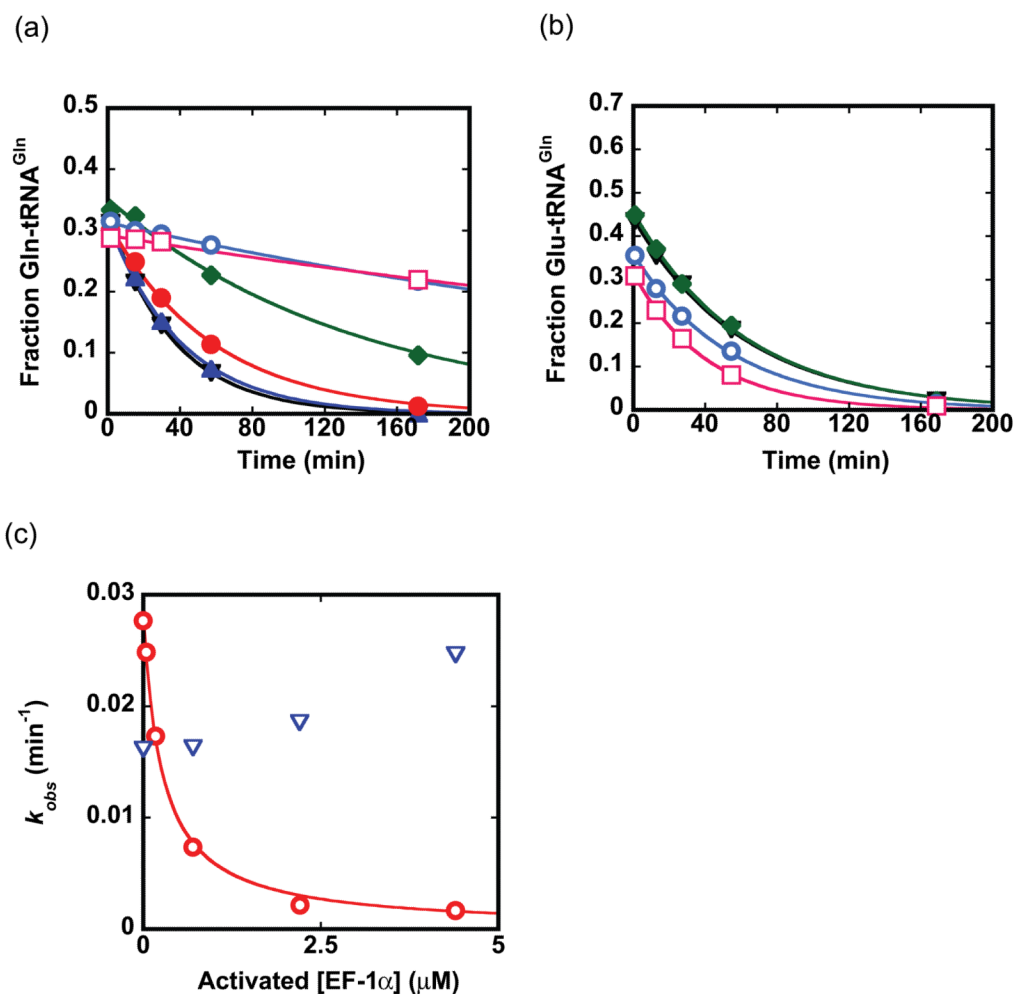
(a)

(b)

(c)

Fig. 7.
Binding affinity of EF-1α to aminoacyl-tRNAs. Decreases in the fraction of Gln-tRNA^{Gln} (a) and Glu-tRNA^{Gln} (b) present over time in the presence of different concentrations of EF-1α at 0 μM (black inverted triangles), 0.044 μM (blue filled triangles), 0.17 μM (red filled circles), 0.7 μM (green filled diamonds), 2.2 μM (cyan circles), and 4.4 μM (pink squares). Each timecourse is fit to an exponential function to derive k_{obs}. (c) Rate constants for protection of spontaneous deacylation in the presence of EF-1α obtained from panels (a) and (b) are replotted and fit to a hyperbolic binding curve to derive the K_d for EF-1α binding to Gln-tRNA^{Gln} (0.29 ± 0.03 μM; red trace). No significant correlation of the rate constant for deacylation of Glu-tRNA^{Gln}, with increasing EF-1α concentration, could be made (blue inverted triangles indicate the data in this case).
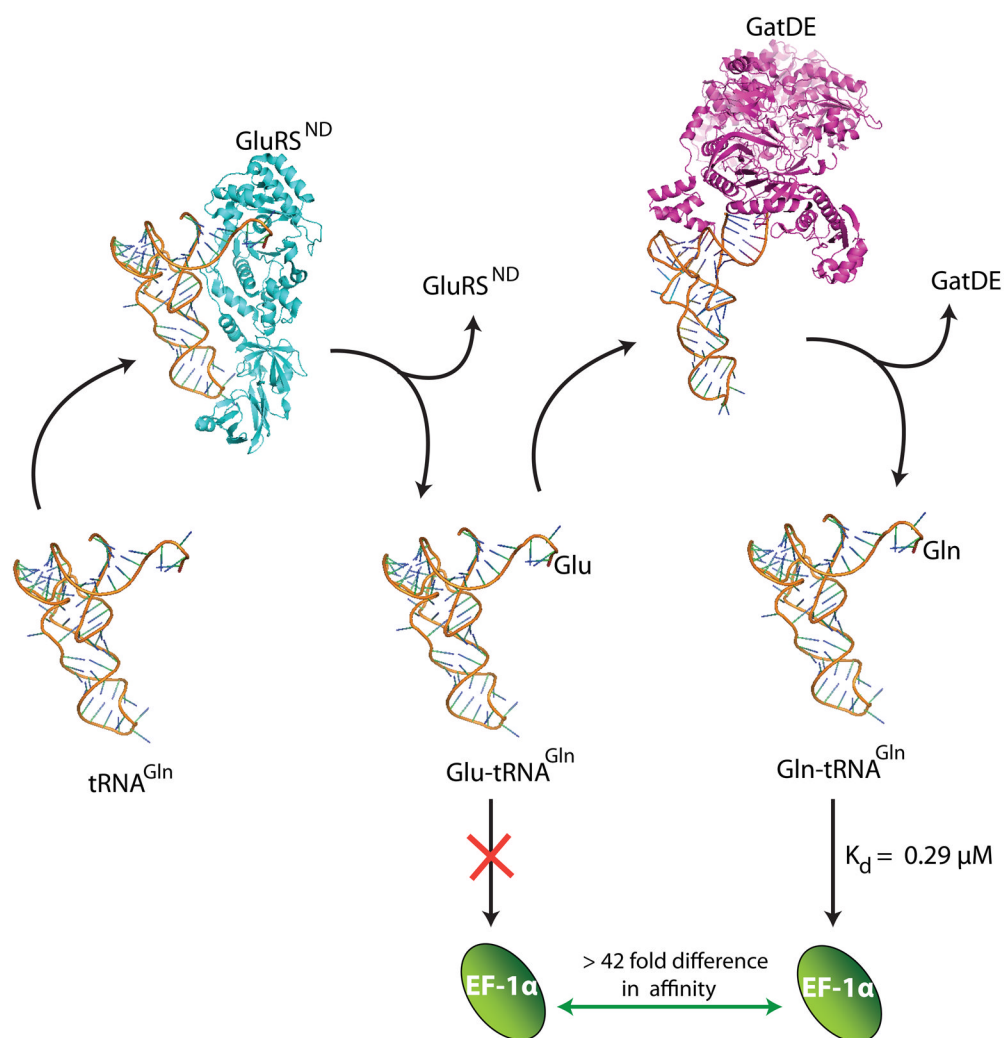
Fig. 8.
Model for two-step synthesis of Gln-tRNA^{Gln} without channeling in Archaea. In this model independent, distributive function of GluRSND and GatDE together with exclusion of Glu-tRNA^{Gln} binding by elongation factor suffices for selective glutamine incorporation in *M. thermautotrophicus*.